

# On the photochemical oxidation of natural trace gases and man-made pollutants in the troposphere

D.H. Ehhalt

*Institut für Atmosphärische Chemie, Forschungszentrum Jülich, Postfach 1913, D-52428 Jülich, Germany*

---

## Abstract

Natural trace gases, as well as anthropogenic pollutants, are mostly emitted as reduced or partly oxidized molecules. In the earth's atmosphere, which contains approximately 20% oxygen, most of these gases will be oxidized and converted to acidic, and therefore water-soluble, species. These are eventually washed out by precipitation or directly deposited on the earth's surface and thus removed from the atmosphere. The atmospheric cycling of the trace gases is not a simple process. Like oxidation in a flame, atmospheric oxidation is mediated by chains of free radical reactions. By far the most important radical in the troposphere is the hydroxyl radical, OH. It is generated photochemically, and reacts with most atmospheric trace gases, in many cases as the first and rate determining step in the reaction chains leading to their oxidation. Usually, these chains regenerate OH, thus maintaining OH at relatively high day-time concentrations in the order of  $10^6/\text{cm}^3$ . At these concentrations OH is by far the most important oxidizing agent in the troposphere. The reactions most important in controlling the local OH concentration are presented. They form the framework of a photochemical reaction system, whose properties are analysed. The OH concentrations predicted from model calculations are compared with measured ones to test the current status of our understanding of the OH chemistry.

*Key words:* Hydroxyl radical; Photochemical oxidation; Removal of atmospheric gaseous pollutants; Self-cleansing of the troposphere

---

## 1. Introduction

In this presentation I address the following question: how does the atmosphere manage to get rid of the gaseous pollutants man injects into it? And how does the atmosphere rid itself from natural emissions? In general terms the answer to these questions appears simple. Natural trace gases, including anthropogenic, are mostly emitted as reduced or partly oxidized molecules. In the earth's atmosphere, which contains about 20% oxygen, most of these gases will be oxidized and converted to acidic, and therefore water-soluble, products. These are eventually washed out by precipitation or directly deposited on the earth's surface and thus removed from the atmosphere. The difficulties are the details of these processes.

The atmospheric oxidation of a given molecule can be quite a complex process. Moreover, depending on the time of day or on altitude it may take different reaction paths. In general, however, the chemical oxidation proceeds via chains of radical reactions.

As it turns out, the most important oxidation reactions in the troposphere, i.e. those that cause the largest chemical turnover of material in the lowest 15 km of the atmosphere, are those initiated by the hydroxyl radical, OH. It is on those reactions that I concentrate in this paper. The OH radical is known to react with most trace gases, in many instances as the first and rate determining step. Thus OH controls the removal, and therefore the tropospheric concentrations, of many trace gases. Since the reaction rate con-

stants are known, all that is required to calculate the atmospheric lifetimes of the trace gases is knowledge of the tropospheric distribution of the OH concentration. This knowledge, however, is not easily gained, because, in turn, all these gases influence the concentration of OH. As a consequence the chemical system controlling the OH concentration is complex with many intricate feedback loops; its complete analysis requires rather complicated numerical models. Fortunately, the essential features of the chemical system can be understood with the help of a few and simple examples, because the dominant reaction pathways follow a limited number of basic patterns.

Thus, below I present a simplified chemical reaction scheme and attempt to derive its basic properties using a numerical example. To test the understanding thus gained we compare model-calculated OH concentrations with the few existing measurements of OH in surface air. It is probably worthwhile to note that much of that understanding is the result of the last 10 years of research.

## 2. Basic features of OH photochemistry

Despite all of the man-made and natural trace gas emissions, the troposphere still represents a system of very dilute fuel; the most abundant reduced molecule, CH<sub>4</sub>, is present at an average mixing ratio of only 1.7 p.p.m. In addition, the system operates at relatively low temperatures, between 200 and 300 K; thus it needs an external source of energy to get its reactions started. That energy is provided by solar radiation at short wavelengths. So photochemistry has to be an important part in our considerations. The solar ultraviolet radiation (UV) available in surface air is characterised in Fig. 1. Its spectral distribution shows a steep cutoff towards shorter wavelengths beginning at about 320 nm. Radiation below 290 nm does not reach the earth's surface. This cutoff is caused by the absorption of solar UV by stratospheric ozone, O<sub>3</sub> (Fig. 1).

A comparison of the spectrum of solar UV at the earth's surface with the absorption cross section of molecular oxygen, O<sub>2</sub>, shows no overlap.

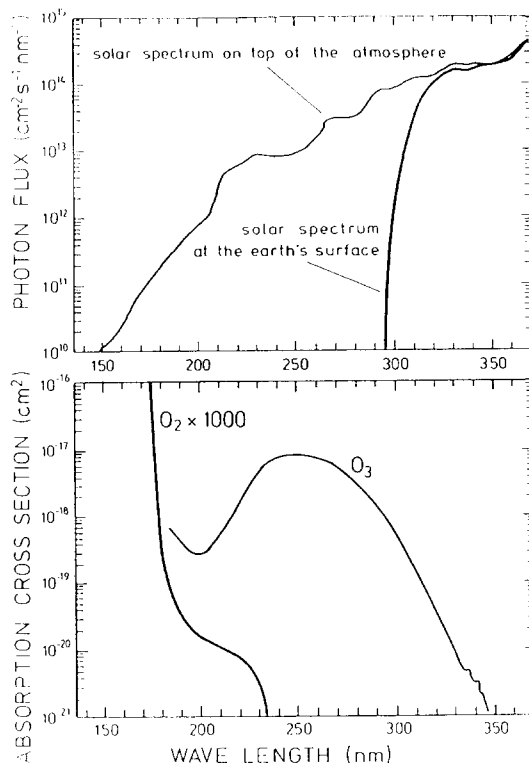


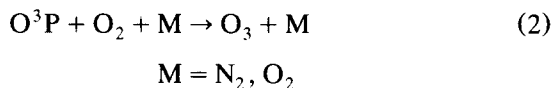
Fig. 1. The spectrum of the ultraviolet component of solar radiation and of the solar radiation reaching the surface of the earth (upper panel). Absorption cross sections of O<sub>2</sub> and O<sub>3</sub>, the two main absorbers of solar UV in the atmosphere (lower panel).

The same is true for the other major constituents of air, N<sub>2</sub>, CO<sub>2</sub>, and H<sub>2</sub>O: the solar photons reaching the troposphere do not have enough energy to photolyse one of the major components of air. However, the radiation is energetic enough to interact with trace gases. Fig. 1, for example, shows a significant overlap between the absorption cross section of O<sub>3</sub> and solar UV at the earth's surface. Indeed, photolysis of O<sub>3</sub> by UV photons,  $h\nu$ , is important. At wavelengths longer than 320 nm, the product is ground state atomic oxygen, O<sup>3</sup>P:



Despite the fact that atomic oxygen is a reactive species, its generation by the reaction in Eq. 1 does not contribute much to the oxidation of

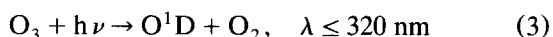
trace gases in the troposphere.  $O^3P$  rapidly recombines with molecular oxygen to form  $O_3$ .



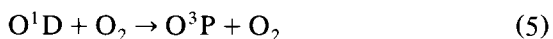
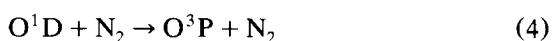
Generation of  $O^3P$  by photolysis (Eq. 1), and loss by recombination (Eq. 2), result in a steady state concentration of about  $10^3$  molecules/cm<sup>3</sup>. Given the relatively low reactivity of  $O^3P$ , that concentration is too small to be of significance for the oxidation of trace gases in the troposphere. The fact that the O atoms generated in the reaction in Eq. 1 interact rapidly with one of the major constituents of air to form the less reactive species  $O_3$  limits their possible importance.

### 2.1. OH Production

Although photolysis of  $O_3$  occurs at a much slower rate at wavelengths below 320 nm than it does at those above, it is much more important for tropospheric chemistry. At those wavelengths the resulting O atom is electronically excited, with an energy of about 2 eV above the ground state:



The major part of the  $O^1D$  atoms produced in the reaction in Eq. 3 is quenched to  $O^3P$  in collisions with atmospheric nitrogen and oxygen molecules:



but when colliding with water vapor molecules,  $H_2O$ , the excited oxygen atoms react to form the very reactive hydroxyl radical, OH:



Because  $H_2O$  is present in surface air in concentrations of up to 1% and because the reaction in Eq. 6 has a rate constant of approximately a factor of 10 higher than the quenching reactions of Eqs. 4 and 5 (see Table 1), up to 10% of the  $O^1D$  generate OH.

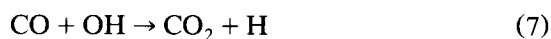
The hydroxyl radical does not react with any of the major constituents of air. However, it has the

ability to initiate chain reactions in an  $O_2$ -containing atmosphere. When reacting with trace gas molecules, OH is not consumed, but is regenerated in catalytic cycles. In this way relatively large OH concentrations, of the order of  $10^6$ /cm<sup>3</sup>, are maintained in the sunlit troposphere despite OH's high reactivity towards most pollutants and other trace gases. These two properties — high reactivity and relatively large concentrations — make OH the most important oxidation agent in the troposphere.

OH is nearly ubiquitous, because  $O_3$  is found virtually everywhere. Even in the remote troposphere  $O_3$  is present as part of a natural cycle which mixes it down from the stratosphere. It is also interesting to note that the spectral region of solar UV that causes  $O^1D$  production coincides closely with that causing sunburn. Thus, a rather trivial experience can tell us where to expect strong OH formation. Obviously the OH concentration will have a strong seasonal and diurnal cycle.

### 2.2. OH Recycling

The simplest example of OH recycling is given by the atmospheric oxidation of carbon monoxide, CO. The reaction of CO with OH quickly forms the stable end product, carbon dioxide,  $CO_2$ :



It also forms a hydrogen atom, H, which is very reactive. The H atom rapidly combines with  $O_2$  to form a hydroperoxy radical,  $HO_2$ :



The addition of an H atom to  $O_2$  weakens the bond between the oxygen atoms, and  $HO_2$  reacts much more readily than  $O_2$ . In particular  $HO_2$  oxidizes nitric oxide, NO:



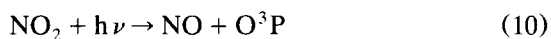
Over middle Europe, where day-time concentrations of NO exceed 0.1 p.p.b., Eq. 9 is by far the fastest  $HO_2$  reaction. Most important for our present argument is the fact that the OH radical consumed in the reaction of Eq. 7 is regenerated in the reaction of Eq. 9.

Table 1:  
Reactions and rate constants used for the calculation of concentrations of OH

A.	Photolytic reactions		Frequency (s <sup>-1</sup> )
	O <sub>3</sub> + hν	→ O <sup>1</sup> D + O <sub>2</sub> , λ ≤ 320 nm	1.1 × 10 <sup>-5</sup>
	NO <sub>2</sub> + hν	→ NO + O	6.5 × 10 <sup>-3</sup>
	CH <sub>2</sub> O + hν	→ CO + H <sub>2</sub>	7.8 × 10 <sup>-5</sup>
	CH <sub>2</sub> O + hν	→ HCO + H	2.0 × 10 <sup>-5</sup>
	H <sub>2</sub> O <sub>2</sub> + hν	→ OH + OH	8.4 × 10 <sup>-6</sup>
B.	Heterogeneous removal (rainout and collision with aerosol particles)		Frequency (s <sup>-1</sup> )
	HNO <sub>3</sub>		1.1 × 10 <sup>-5</sup>
	H <sub>2</sub> O <sub>2</sub>		1.1 × 10 <sup>-5</sup>
C.	Gas phase reactions		Rate constant (cm <sup>3</sup> /s)
	O <sup>1</sup> D + H <sub>2</sub> O	→ OH + OH	2.2 × 10 <sup>-10</sup>
	O <sup>1</sup> + N <sub>2</sub>	→ O <sup>3</sup> P + N <sub>2</sub>	2.6 × 10 <sup>-11</sup>
	O <sup>1</sup> D + O <sub>2</sub>	→ O <sup>3</sup> P + O <sub>2</sub>	4.0 × 10 <sup>-11</sup>
	OH + O <sub>3</sub>	→ HO <sub>2</sub> + O <sub>2</sub>	7.0 × 10 <sup>-14</sup>
	OH + H <sub>2</sub> O <sub>2</sub>	→ HO <sub>2</sub> + H <sub>2</sub> O	1.7 × 10 <sup>-12</sup>
	OH + H <sub>2</sub>	→ H + H <sub>2</sub> O	6.7 × 10 <sup>-15</sup>
	OH + NO <sub>2</sub> + M	→ HNO <sub>3</sub> + M	1.1 × 10 <sup>-11</sup>
	OH + CO	→ H + CO <sub>2</sub>	2.4 × 10 <sup>-13</sup>
	OH + CH <sub>4</sub>	→ CH <sub>3</sub> + H <sub>2</sub> O	7.7 × 10 <sup>-15</sup>
	OH + CH <sub>2</sub> O	→ HCO + H <sub>2</sub> O	1.0 × 10 <sup>-11</sup>
	OH + CH <sub>3</sub> O <sub>2</sub> H	→ CH <sub>3</sub> O <sub>2</sub> + H <sub>2</sub> O	1.0 × 10 <sup>-11</sup>
	OH + OH	→ H <sub>2</sub> O + O	1.9 × 10 <sup>-12</sup>
	OH + OH + M	→ H <sub>2</sub> O <sub>2</sub> + M	3.8 × 10 <sup>-12</sup>
	OH + HO <sub>2</sub>	→ H <sub>2</sub> O + O <sub>2</sub>	6.8 × 10 <sup>-11</sup>
	OH + SO <sub>2</sub> + M	→ HSO <sub>3</sub> + M	8.9 × 10 <sup>-13</sup>
	H + O <sub>2</sub> + M	→ HO <sub>2</sub> + M	1.2 × 10 <sup>-12</sup>
	HO <sub>2</sub> + O <sub>3</sub>	→ OH + O <sub>2</sub> + O <sub>2</sub>	2.0 × 10 <sup>-15</sup>
	HO <sub>2</sub> + HO <sub>2</sub>	→ H <sub>2</sub> O <sub>2</sub> + O <sub>2</sub>	1.6 × 10 <sup>-12</sup>
	HO <sub>2</sub> + HO <sub>2</sub> + M	→ H <sub>2</sub> O <sub>2</sub> + O <sub>2</sub> + M	1.2 × 10 <sup>-12</sup>
	HO <sub>2</sub> + NO	→ OH + NO <sub>2</sub>	8.2 × 10 <sup>-12</sup>
	HO <sub>2</sub> + CH <sub>3</sub> O <sub>2</sub> + M	→ CH <sub>3</sub> O <sub>2</sub> H + M	5.9 × 10 <sup>-12</sup>
	O + O <sub>2</sub> + M	→ O <sub>3</sub> + M	1.4 × 10 <sup>-14</sup>
	O <sub>3</sub> + NO	→ NO <sub>2</sub> + O <sub>2</sub>	1.8 × 10 <sup>-14</sup>
	HCO + O <sub>2</sub>	→ CO + HO <sub>2</sub>	5.5 × 10 <sup>-12</sup>
	CH <sub>3</sub> + O <sub>2</sub> + M	→ CH <sub>3</sub> O <sub>2</sub> + M	1.1 × 10 <sup>-12</sup>
	NO <sub>2</sub> + O <sub>3</sub>	→ NO <sub>3</sub> + O <sub>2</sub>	3.4 × 10 <sup>-17</sup>
HSO <sub>3</sub> + O <sub>2</sub>	→ HO <sub>2</sub> + SO <sub>3</sub>	4.0 × 10 <sup>-13</sup>	
CH <sub>3</sub> O <sub>2</sub> + NO	→ CH <sub>3</sub> + NO <sub>2</sub>	7.6 × 10 <sup>-12</sup>	
CH <sub>3</sub> O <sub>2</sub> + O <sub>2</sub>	→ HO <sub>2</sub> + CH <sub>2</sub> O	1.5 × 10 <sup>-15</sup>	

Rates of photolytic processes were measured on 20 May 1983, 09:08–11:30 h, at Deuselbach, Hunsrück, Germany. Rate constants for the gas phase reactions are given for 298 K temperature and 1 atm pressure (DeMore et al., 1985). Three body reactions are described by quasi-bimolecular rate constants.

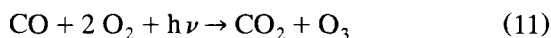
It is also important to note that the nitrogen dioxide molecule, NO<sub>2</sub>, generated in the reaction in Eq. 9 photolyses readily in the near UV and thus contributes to tropospheric photochemistry:



In the sunlit atmosphere the lifetime of NO<sub>2</sub> against photolysis is a few minutes (see Table 1). The resulting O atom immediately combines with O<sub>2</sub> to form O<sub>3</sub> (Eq. 2).

Supplemented by the reactions in Eqs. 10 and 2 the hydroxyl radical reactions in Eqs. 7–9 com-

bine to oxidize CO to CO<sub>2</sub> without consuming OH, HO<sub>2</sub>, NO and NO<sub>2</sub>. The reaction can be summarised:

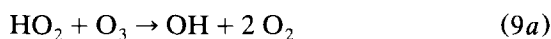


Because OH and HO<sub>2</sub> (NO and NO<sub>2</sub>) are not consumed in the catalytic oxidation of CO to CO<sub>2</sub>, the cycle consisting of the reactions in Eqs. 7–10 and 2 can be completed repeatedly before that chain reaction is interrupted by termination reactions.

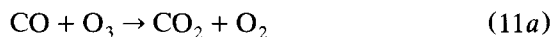
It is probably also worthwhile to point out that O<sub>3</sub> is formed in that chain reaction. Thus this simple cycle already contains the most essential element of photochemical smog formation: a partly reduced gas, CO, is photochemically oxidized via hydroxyl radicals. In the presence of NO, ozone is formed — at a ratio of one O<sub>3</sub> molecule per CO molecule consumed.

By this and other chain reactions OH and HO<sub>2</sub> are interconverted within a matter of seconds. Thus, both are often put together and designated HO<sub>x</sub>. Similarly the sum of NO and NO<sub>2</sub> is often designated NO<sub>x</sub>.

Using the atmospheric removal of CO by OH we can also understand another property of the atmospheric reaction system, namely its control by NO<sub>x</sub>. Besides the reaction in Eq. 9 there is another reaction which converts HO<sub>2</sub> back to OH:



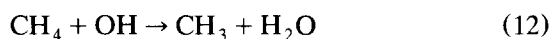
Even if there were no NO present the reaction in Eq. 9a would close the CO oxidation chain. But in that case the chain would consist of the reactions in Eqs. 7, 8 and 9a and the net result would be



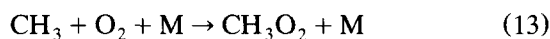
The oxidation of CO in an NO<sub>x</sub>-free atmosphere leads to the destruction of O<sub>3</sub>, whereas it led to a production while NO<sub>x</sub> was present. This is just another example for the fact that the tropospheric production of O<sub>3</sub> is linked to the presence of NO<sub>x</sub>. Since the rate constant in the reaction in Eq. 9 is 4000 times larger than that in the reaction in Eq. 9a, the crossover from O<sub>3</sub> destruction to O<sub>3</sub> production begins at an NO

mixing ratio of about 10 p.p.t. That value is nearly always exceeded in the heavily populated and industrialized northern mid-latitudes. Indeed, all evidence points to a doubling of the tropospheric O<sub>3</sub> concentrations at these latitudes over the last 40 years, triggered mainly by the increase in NO<sub>x</sub> emissions.

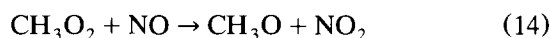
Some of the HO<sub>x</sub> catalysed oxidation reactions have another interesting property. At the relatively large NO<sub>x</sub> concentrations of northern mid-latitudes they produce a gain in HO<sub>x</sub>. The simplest example is the oxidation of methane, CH<sub>4</sub>, which is also initiated by the OH radical.



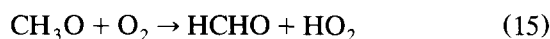
OH abstracts an H atom to form a water molecule, H<sub>2</sub>O, while the remaining methyl radical, CH<sub>3</sub>, reacts extremely rapidly



Like the H atom in the reaction in Eq. 8 it combines with O<sub>2</sub> to form a peroxy radical, the methylperoxy radical, CH<sub>3</sub>O<sub>2</sub>. And similarly to HO<sub>2</sub>, CH<sub>3</sub>O<sub>2</sub> oxidizes NO to NO<sub>2</sub>:



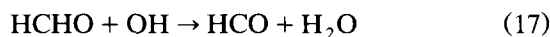
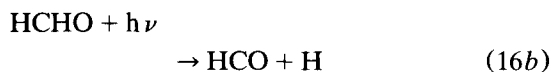
The resulting methoxy radical CH<sub>3</sub>O reacts rapidly with O<sub>2</sub> to give formaldehyde, HCHO:



The HO<sub>2</sub> also formed in the reaction in Eq. 15 reacts back to OH via the reaction in Eq. 9 which closes the HO<sub>x</sub> radical cycle.

Formaldehyde is the first intermediate product of CH<sub>4</sub> oxidation with a lifetime longer than a few seconds. In the sunlit atmosphere it lives around 5 h and thus can reach concentrations of about 0.5 p.p.b., even in unpolluted air. It is also subject to transport, whereas all the preceding radical type intermediates react virtually at the location of the primary OH attack of CH<sub>4</sub>.

Formaldehyde is eventually removed by photolysis; it also reacts with OH.



The formyl radical, HCO, formed in the reactions in Eqs. 16*b* and 17, reacts rapidly with O<sub>2</sub>:



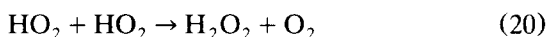
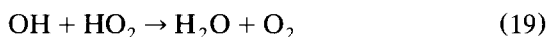
where the HO<sub>x</sub> radical destroyed in the reaction in Eq. 17 is regenerated. Moreover, additional HO<sub>x</sub> is generated from HCO and H formed in the photolysis of HCHO (Eq. 16*b*). This channel becomes important in the photolysis of HCHO at shorter wavelengths (beginning at 340 nm), and contributes about 15% to the removal of HCHO at ground level. Consequently, since HCO and H are rapidly converted to HO<sub>2</sub>, about 0.3 additional HO<sub>x</sub> molecules are formed in the oxidation of one CH<sub>4</sub> molecule.

Thus, the oxidation of CH<sub>4</sub> in an atmosphere with sufficient NO<sub>x</sub> leads to a net gain of HO<sub>x</sub>; about 25% more HO<sub>x</sub> molecules are returned in the form of HO<sub>2</sub> than are consumed in the form of OH.

CH<sub>4</sub> oxidation in an NO<sub>x</sub>-rich atmosphere acts as a radical amplifier (the inverse is true in an NO<sub>x</sub>-poor environment). Other hydrocarbons show a similar effect on HO<sub>x</sub>.

### 2.3. HO<sub>x</sub> destruction

So far we have dealt with reactions of OH radicals and molecules. Those reactions conserve HO<sub>x</sub>. The ensuing chain reactions merely interconvert OH into HO<sub>2</sub>. To produce a net loss of HO<sub>x</sub> radicals and terminate the reaction chains, HO<sub>x</sub> radicals have to react with other radicals. Reactions of that kind are:



which are responsible for HO<sub>x</sub> radical loss in clean air. The addition of OH to NO<sub>2</sub> forming a nitric acid molecule, HNO<sub>3</sub>,



is the dominant HO<sub>x</sub> loss reaction in the polluted atmosphere.

### 2.4. Quantitative analysis of the HO<sub>x</sub> reaction cycle

The reactions in Eq. 1–21 allow reasonably

accurate estimates of tropospheric OH concentrations. Of course, the chemical system is incomplete and greatly simplified. For instance, in polluted air the low molecular weight non-methane hydrocarbons (NMHC) would have to be included. But the most important reactions have been considered and the essential features of the HO<sub>x</sub> recycling can be reproduced. To estimate the OH concentration we investigated tropospheric air masses in which the concentrations of OH and the most important trace gases, interacting with OH, have been measured. An example of such a data set is given in Table 2. During that experiment which was carried out on 20 May 1983, 09:08–11:30 h, at Deuselbach, a rural station in the Hunsrück mountains, Germany, the photolysis rates were also determined (Perner et al., 1987). They are shown together with the rate constants for the reactions in Eqs. 2–21 in Table 1. With these parameters and the concentrations from Table 2 the local air mass is sufficiently characterised to use our simplified chemical system to calculate the OH and HO<sub>2</sub> concentrations. The results are shown in Fig. 2 which also contains the most important reaction pathways and their conversion rates. Photolysis, Eq. 3, followed by the reaction in Eq. 6, constitutes the main source of HO<sub>x</sub> radicals. Another, but much smaller supply comes from the photolysis of

Table 2:

Concentration of trace gases that interact with and control the concentration of OH, for 09:08–11:30 h, 20 May 1983, at Deuselbach, Hunsrück, Germany

Trace gas	Mixing ratio (p.p.b.)	Concentration (cm <sup>-3</sup> )
O <sub>3</sub>	53	1.32 × 10 <sup>12</sup>
H <sub>2</sub> O	9.1 × 10 <sup>6</sup>	2.27 × 10 <sup>17</sup>
CO	260	6.5 × 10 <sup>12</sup>
CH <sub>4</sub>	1740	4.4 × 10 <sup>13</sup>
H <sub>2</sub>	600	1.5 × 10 <sup>13</sup>
SO <sub>2</sub>	1.6	4 × 10 <sup>10</sup>
NO	0.5	1.3 × 10 <sup>10</sup>
NO <sub>2</sub>	1.6	4 × 10 <sup>10</sup>
CH <sub>2</sub> O	0.5	1.3 × 10 <sup>10</sup>

The mixing ratio expresses the concentration of a trace gas relative to the total concentration of air molecules.

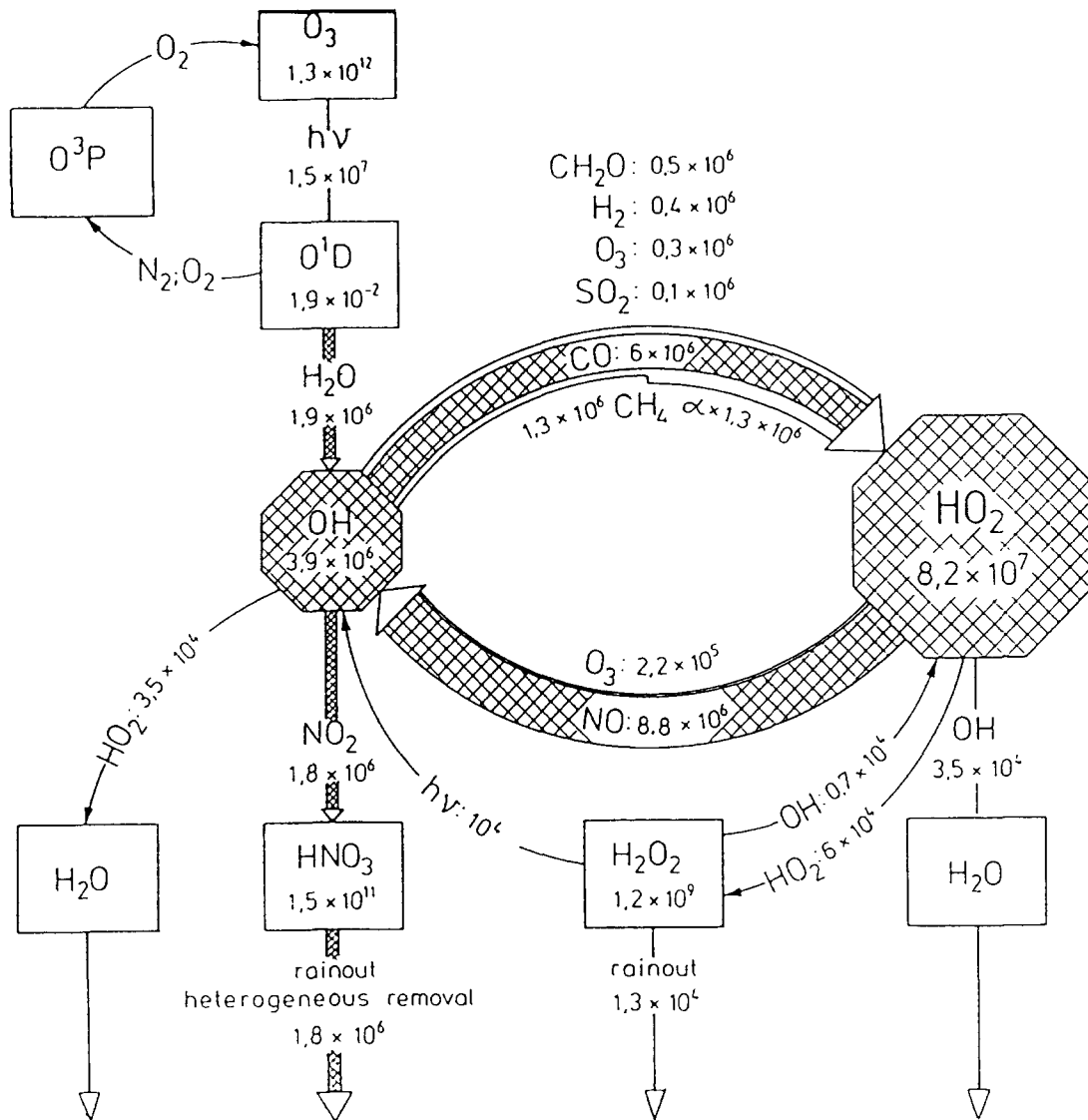


Fig. 2. Reaction cycle of OH and HO<sub>2</sub>. The calculation simulates an air mass observed between 09:08 h and 11:30 h, 20 May 1983 at Deuselbach (see Tables 1 and 2). Numbers in boxes are calculated concentrations (cm<sup>-3</sup>); numbers on arrows are the conversion rates of HOx (cm<sup>-3</sup> per s) resulting from reactions with the relevant trace gases (from Ehhalt et al., 1991).

HCHO which in the present situation is derived mostly from CH<sub>4</sub> oxidation. It is indicated by the factor  $\alpha$  in Fig. 2.

In the steady state that net production of HOx is balanced by a net destruction. As mentioned before, the main loss of HOx is via the addition the reaction in Eq. 21 of OH to NO<sub>2</sub>. In the present example less than 10% of the HOx loss is

contributed by the reactions in Eqs. 19 and 20 of HO<sub>2</sub> with OH and HO<sub>2</sub>, respectively. The fact that essentially all of the HOx production and destruction proceeds via the OH radical simplifies significantly the calculation of the OH concentration. It means that the interconversion fluxes of OH to HO<sub>2</sub> and vice versa nearly cancel each other out. Consequently the OH concentration

can be estimated in first approximation from a single balance-equation consisting of the primary OH production from  $O_3$  photolysis and net destruction by  $NO_2$ . Such an estimate would lead to a OH concentration of  $4.3 \times 10^6/cm^3$  compared with the  $3.9 \times 10^6/cm^3$  calculated from the simplified model (Eqs. 1–21) whose results are shown in Fig. 2. Both values are close to the OH concentration of  $5.1 \times 10^6/cm^3$  which is calculated from a time-dependent box model including the effect of light non-methane hydrocarbons, NMHC (Perner et al., 1987). It should be noted, however, that the present example was selected for its low NMHC concentrations, thus keeping their influence on the OH concentration relatively small.

Despite the large net destruction of OH by  $NO_2$  most of the OH is interconverted to  $HO_2$  with the largest contribution coming from the CO oxidation. The sum of all conversion rates amounts to  $9 \times 10^6/cm^3$  per s. (An additional 20% would have been contributed by the NMHC, had they been included.) It follows that a HOx radical is recycled five times before the chain is terminated by the loss reaction in Eq. 21 which proceeds at a rate of  $1.8 \times 10^6$  OH/ $cm^3$  per s. That value is fairly typical for the recycling ratio; in most situations model predictions deviate less than a factor of 2 from that ratio.

The corresponding time constants are obtained by dividing the concentrations by the rates. Thus, a HOx radical is recycled every 9 s and the mean lifetime of a HOx radical is 45 s. The data in Fig. 2 allows the impact on OH concentrations of concentration changes of different trace gases to be estimated. Of particular interest is the change in the  $NO_2$  concentration which is accompanied by a similar change in NO and therefore influences the OH concentration in two different and counteracting ways. At very small NOx concentrations the recycling of  $HO_2$  with NO to OH through the reaction in Eq. 9 determines the impact of NOx on OH, because OH loss through the reaction in Eq. 21 with  $NO_2$  becomes negligible compared with the reactions in Eqs. 19 and 20 between the HOx radicals. Consequently, an increase in the NO concentration leads to a faster conversion of  $HO_2$  to OH and thus to a higher OH concentration because the simultaneous in-

crease of  $NO_2$  leads to an insignificant increase in the loss of OH. The converse is true with large concentrations of NOx. In that case, reaction 21 with  $NO_2$  is the dominant loss of HOx. Further increases in  $NO_2$  concentrations cause corresponding decreases in the HOx concentrations. Because of the large NO concentration and consequent rapid conversion of  $HO_2$  to OH, the  $HO_2$  concentration is low. A change of the OH: $HO_2$  ratio can no longer absorb the HOx losses and they carry over to a reduction in OH concentration. This dependence of HOx and OH concentrations on  $NO_2$  concentrations is shown in Fig. 3. The maximum in the OH profile resulting from the two counteracting NOx influences is clearly visible; it occurs at an  $NO_2$  concentration of 0.5 p.p.b. At an  $NO_2$  concentration of 10 p.p.b. the OH concentration would drop by about a factor of 10 below its maximum value. Fig. 3 demonstrates clearly the non-linear response of the OH concentrations to changes in the NOx concentration. At the same time it demonstrates that the calculated OH concentration is relatively robust against changes in NOx. Over a wide range of  $NO_2$  concentrations, from 0.001 p.p.b. to 1 p.p.b., the calculated OH concentration changes less

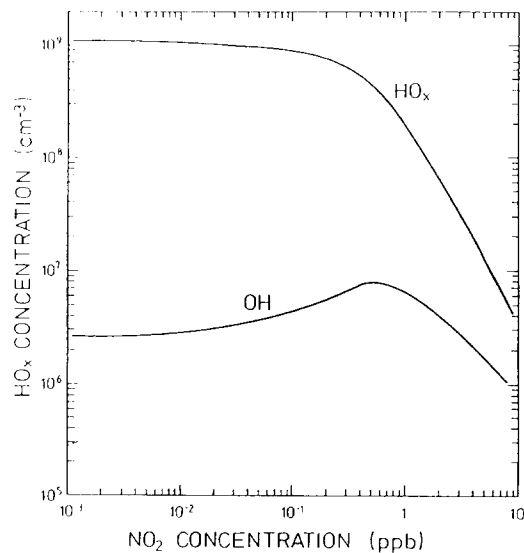


Fig. 3. The dependence of concentrations of OH and HOx on those of  $NO_2$ . The other parameters were fixed to the values observed on 20 May 1983 at Deuselbach.

than a factor of 3. On the other hand a large emission of  $\text{NO}_x$  can significantly perturb the chemical system of the local atmosphere. In such a situation the atmospheric OH concentration is significantly lowered and the capacity of the local atmosphere to degrade trace gases and pollutants would be greatly reduced. As a consequence, a larger part of the emitted pollutants is expected to spill over into the surrounding environment.

Another example is the influence on OH exerted by CO. It is shown in Fig. 4. At  $\text{NO}_2$  mixing ratios below 1 p.p.b. its increase leads to a lowering of OH due to the faster conversion of OH to  $\text{HO}_2$ . In fact, model calculations predicted a decrease of the global average OH concentration as a consequence of the observed increase in CO in the northern hemisphere of  $\sim 1\%$ /year (Thompson and Cicerone, 1986).

The example presented further demonstrates that the concentration of OH may be determined by a relatively small number of reactions despite OH's many interactions and feedback loops. This is especially true for rural and remote environments. The important reactions are obviously those providing the fastest local conversion rates, i.e. those which show high rate constants and whose 'reactands' are present in large concentrations. They form a central chemical reaction system which establishes a certain OH concentration which is then available for the removal of other trace gases. Because of their comparatively smaller conversion rates the other gases provide little feedback to OH concentrations.

### 3. Comparison of model predicted OH concentrations with measurements

To test our understanding of the chemical system controlling OH as developed in the previous section, it is necessary to have measurements of tropospheric OH concentrations along with measurements of those parameters and trace gas concentrations which are known to determine OH.

Very few such measurements exist. To our knowledge the group of the Institute of Atmospheric Chemistry at Jülich is the only one to have made simultaneous measurements of OH

and relevant support parameters. One example is quoted in Tables 1 and 2; others can be found in Perner et al. (1987), Platt et al. (1988), Dorn et al. (1988), and Callies (1988). The techniques for measuring the trace gases are also found in these publications and the references therein. The method used for measuring the photolysis rates has been published by Junkermann et al. (1989).

OH was measured using long-path absorption spectroscopy. The light source consisted of a mode-locked argon ion laser which pumped a frequency-doubled dye laser. It emitted a broad line at 308 nm encompassing the strong  $Q_1(2)$  and the weaker  $Q_{21}(2)$  line of the OH absorption spectrum. At Jülich in 1987 the  $Q_1(3)$  and  $P_1(1)$  lines were observed. The OH absorption signal superimposed on the laser light after a 5- to 10-km passage through the troposphere was resolved by a double monochromator with a mechanical scanning system — since 1986 with a photodiode array — and recorded by an electronic data collection system. The method, calibration, data handling, and accuracy have been described by Hübler et al. (1984), and the more recent modifications of the system by Callies (1988), and Dorn et al. (1988). To account for the proper shape of the OH absorption lines (Callies, 1988; Callies et al., unpublished data), the OH measurements shown in this contribution have been corrected by a factor of 1.14, against those published.

The measurements were made in different concentration domains of  $\text{NO}_x$  and non-methane hydrocarbons, NMHC. The OH measurements in 1983 at Deuselbach, a rural station at an altitude of 480 m, and in 1984 at Schauinsland, a mountain station in the Black Forest about 1300 m above sea level, were made in conditions with relatively small  $\text{NO}_2$  and NMHC concentrations. They tend to fall in a band of ethene concentrations between 0.3 and 1 p.p.b. and  $\text{NO}_2$  concentrations of 0.4–2 p.p.b., i.e. just covering the maximum of the predicted OH concentration surface (see Fig. 3). The OH measurements at Jülich were made in a moderately industrialised area during periods with larger concentrations of NMHC and  $\text{NO}_2$ , the latter varying between 2

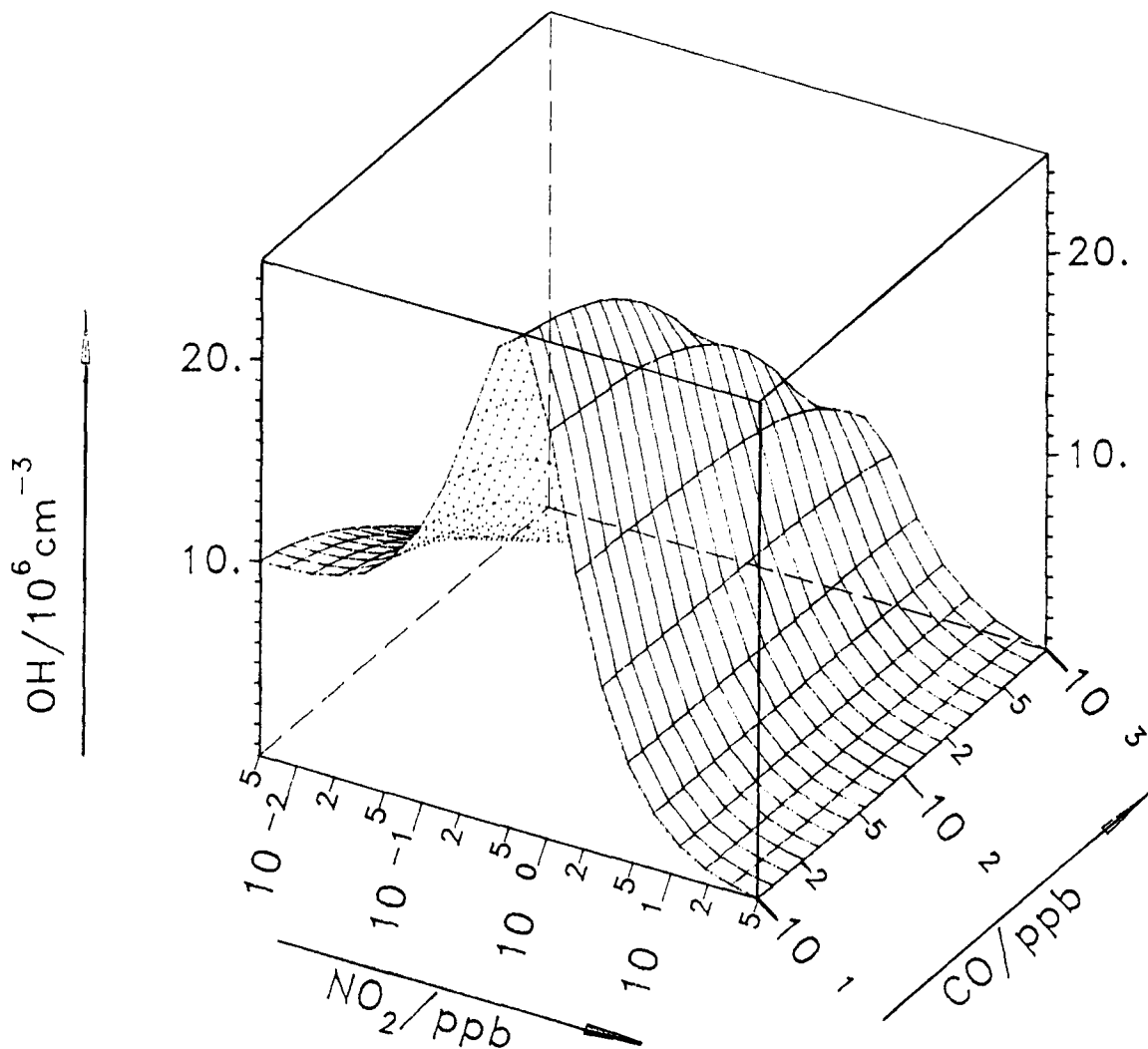


Fig. 4. The dependence of calculated OH concentrations on different mixtures of  $\text{NO}_2$  and CO for typical values of the other precursors. The calculations were performed with the gas phase mechanism of the RADM II (Regional Acid Deposition Model).

and more than 10 p.p.b. Thus, they cover the right hand flank of the predicted OH concentrations. Ethene concentrations varied between 0.5 and several p.p.b.

Obviously the small amounts of NMHC found in the Schauinsland and Deuselbach measurements conform more closely to the range over which the simplified model can be considered valid. Fig. 5 shows a diurnal cycle of OH at Schauinsland site (adapted from Platt et al., 1988). The measured OH concentrations show a maxi-

mum close to 12:00 h which correlates well with the measured  $\text{O}_3$  photolysis frequency for the reaction in Eq. 3,  $J_3(\text{O}_3)$ , which determines the primary production of OH. In fact, this correlation provides the dominant dependence of the measured (and predicted) OH concentrations on any of the measured OH controlling parameters. This is shown more clearly in Fig. 6, in which the measured OH concentrations are plotted against the measured photolysis frequency,  $J_3(\text{O}_3)$ . The correlation coefficient,  $r$ , derived from these data

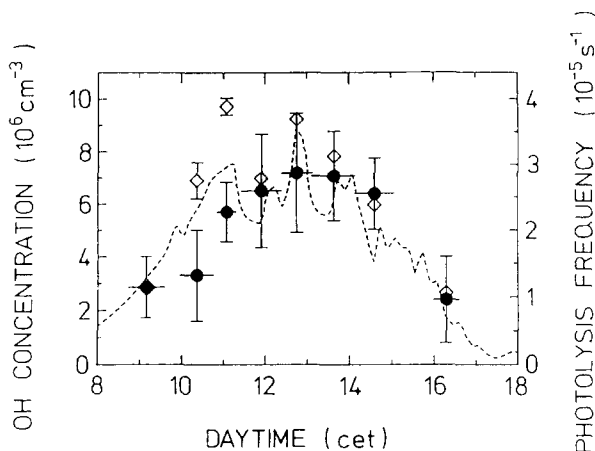


Fig. 5. Diurnal variation of the measured OH concentration (●) and  $O_3$  photolysis frequency  $J_3(O_3)$  at Schauinsland, 25 June 1984. The diamonds indicate the OH concentration calculated with RADM II using the locally measured trace gas concentrations and photolysis rates. The error bars represent the mean standard deviations. To maintain clarity the error bars for the calculated OH concentration are omitted where they would overlap with the experimental uncertainties.

is 0.76. In a probabilistic sense  $r^2$  can be interpreted as the fraction of the total variation in OH which can be explained by the least squares regression line between OH and  $J_3(O_3)$  which is also shown in Fig. 6 (see, Spiegel, 1975). In other

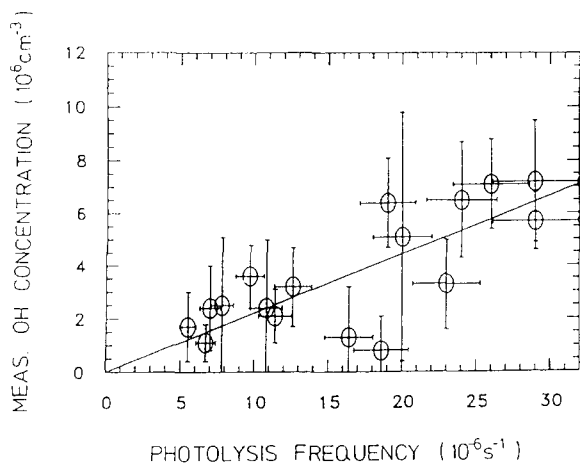


Fig. 6. Correlation of measured OH concentrations with simultaneously observed frequencies of  $O_3$  photolysis,  $J_3(O_3)$  (data from Deuselbach in 1983 and Schauinsland in 1984). Error bars indicate mean standard deviation. The straight line represents a least squares fit through the data and the origin. Correlation coefficient = 0.76 (Ehhalt et al., 1991).

words,  $0.76^2$  or roughly 60% of the observed variation in OH concentration is explained by the variation in  $J_3(O_3)$ .

The remaining variance has to be attributed to the experimental uncertainty of OH, that of  $J_3(O_3)$ , and the influence of the other precursors and parameters on the OH concentration. The latter will be accounted for in the model calculations of OH concentrations. These were based on the chemical mechanism developed for the 'regional acid deposition model', RADM II, which incorporates all the important inorganic reactions and treats NMHC in simplified reactions (Stockwell et al., 1990). It was designed for rural and polluted environments and is therefore applicable to all three of our experimental measurement sites. Fig. 7 shows the correlation between measured and calculated OH concentrations at Deuselbach and Schauinsland. The correlation is quite good, yet the correlation coefficient is only 0.74, i.e. no better than the correlation between the measured OH concentration and  $J_3(O_3)$ : utilising all the supportive data with the model it has not been possible to account for more of the variance in measured concentrations of OH. Most likely a large part of the remaining variance has to be attributed to experimental uncertainties, largely in the measurement of OH.

In view of the experimental uncertainties, Fig. 7 shows a reasonable degree of agreement between the experimental and calculated OH concentrations. There is, however, a tendency for the model to over-predict the OH concentration. The slope of a linear regression line forced to go through the origin is  $0.71 \pm 0.07$ . That corresponds to an average over-prediction of about 30% and suggests a systematic discrepancy, part of which has to be attributed to the possibly systematic errors in the support parameters and rate constants utilised in the calculation of OH concentrations.

The comparison between measured and calculated OH concentrations in the more polluted environment of Jülich reveals greater differences (Fig. 8). The current data set is more complete than the one presented in Ehhalt et al., 1991. At the same time some of the previous uncertainties

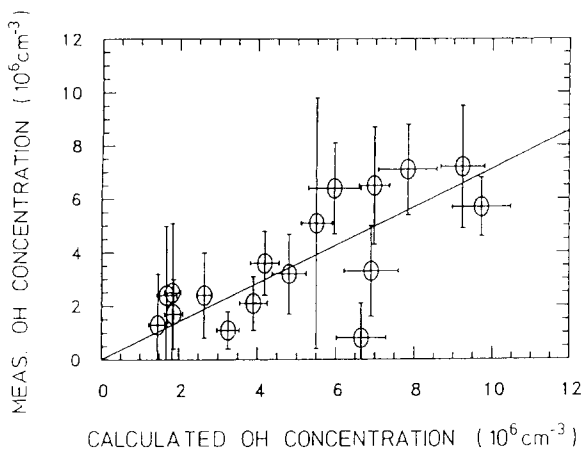


Fig. 7. Correlation of measured and calculated concentrations of OH at Deuselbach in 1983 and Schauinsland in 1984. The error bars represent the mean standard deviations, the straight line a least square fit through the data and the origin. Correlation coefficient = 0.74.

have been improved, notably that of  $J(O_3)$  whose measurement has been carefully recalibrated. A number of the additional measurements range around the detection limit, which varied between 1 and  $2 \times 10^6/\text{cm}^3$ . As expected some of these assume negative values. Like the previous smaller data set the present Jülich data show a larger scatter than the rural measurements. Correspondingly, the correlation between measured and cal-

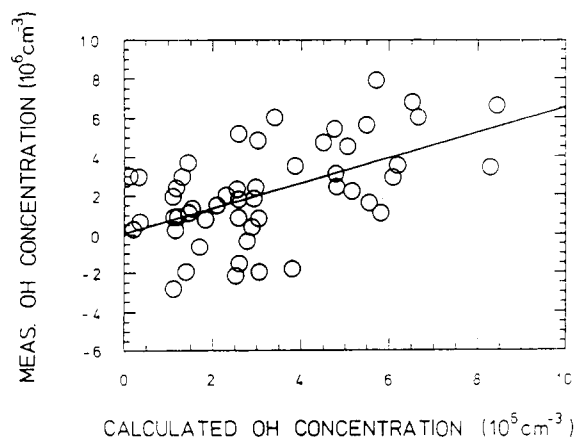


Fig. 8. Correlation of measured and calculated concentrations of OH at Jülich (1987 and 1988). The error bars represent the mean standard deviations. Correlation coefficient, 0.54.

culated OH is weaker with a correlation coefficient,  $r = 0.54$ . This, however, is significantly better than for the previous Jülich data set which essentially showed no correlation. The tendency of the model to over-predict the OH concentration is somewhat larger for the more polluted environment. This is caused by a subset of cases where the model predicts large concentration of OH whereas the measured concentrations were small. A similar behaviour was observed by Perner et al. (1987) from a set of Deuselbach and Jülich data (not included here). The slope of a regression line fitted to the data points in Fig. 8 is  $0.64 \pm 0.14$ . The average calculated OH concentration is  $3.6 \times 10^6/\text{cm}^3$  versus  $2 \times 10^6/\text{cm}^3$  for the mean of the OH measurements, i.e. an over-prediction of about a factor of 1.8, similar to the value of 1.7 which had been deduced before (see Ehhalt et al., 1991).

It is interesting to speculate what kind of process is responsible for the lack of agreement in Fig. 8. Perner et al. (1987) surmised that the reaction of peroxy radicals on aerosol surfaces could possibly explain part of the difference between model led and measured OH concentrations (see also, Mozurkewich et al., 1987). This explanation cannot be invoked in relation to the data sets presented in this contribution. During the periods of OH measurements, which require good visibility, the aerosol content of the atmosphere was low. This was confirmed by simultaneous measurements with an integrating nephelometer whose signals measure the surface area provided by the atmospheric aerosol. Moreover, the measured OH concentration is not correlated with the measured nephelometer signal, another indication that radical loss to aerosol particles was unimportant (Ehhalt, 1989). This does not, of course, exclude the possibility of such losses when there are heavy loads of atmospheric aerosols.

One process which tends to lower the OH concentration is the formation of radical reservoir species. Of particular interest here is the formation of peroxyacetylnitrate, PAN, or similar substances. PAN is sufficiently long-lived to be affected by transport in, and out, of the observation volume. It could thus contribute to a local radical loss because PAN is typically produced in the

atmosphere close to the ground; part of the PAN production is 'lost' by vertical transport. Direct evidence is not available since PAN was not measured when field measurements were made at Jülich in 1987. However, measurements of PAN in later and earlier years showed diurnal variations of not more than 1 p.p.b. amplitude which were reasonably simulated by our model, so indicating that inadequate modelling of PAN is unlikely to explain the entire difference between modelled and measured concentrations of OH at Jülich.

Another possible cause for the discrepancy is the presence of gases not measured and therefore not included in the model calculations. Measurements in rural and urban environments of the Eastern USA, for example, have shown high concentrations of natural hydrocarbons, e.g. isoprene at a few p.p.b. (Martin et al., 1991). The presence of isoprene or other reactive volatile organic carbon species in concentrations observed there could explain the present deviations between model calculated and measured OH abundances.

Finally we have to consider the possibility that a box model is not applicable under the environmental conditions in Jülich. In contrast to the fairly uniform environment at Deuselbach and Schauinsland, the site in Jülich is rather non-uniform with respect to pollutant sources. Spatial homogeneity is not always experienced by the air parcels passing the experimental site. In this case, the steady-state approximation, which requires constant precursor concentrations and meteorological conditions within the parcel over several chemical relaxation times, is no longer valid. For Jülich, however, this consideration would mainly apply to the NO emission from automobile traffic and would cause the model to underestimate the OH — contrary to the present finding.

Therefore, at present we cannot identify a clear cause for the discrepancy between modelled and measured OH concentrations at Jülich.

In summary, it seems from our measurements that models can reasonably simulate the OH concentration in clean environments; they seem less able to explain the measurements in more polluted environments, where they tend to over-pre-

dict. Nevertheless, even there, over-prediction is less than a factor of 2 which is not a bad achievement.

#### 4. Removal of trace gases by OH

Despite the discrepancies with the model results, there is sufficient evidence showing that OH is present in large enough concentrations to make OH by far the most important oxidizing agent in the troposphere. Table 3 summarises a few examples of the tropospheric removal of trace gases by OH including that of CO which, quantitatively, is the most important. The mechanism of CO oxidation in the troposphere has already been discussed; it exclusively proceeds through reaction with OH. In addition, a small fraction of tropospheric CO, less than 10%, is taken up by soil micro-organisms and thus removed from the atmosphere. Similar arguments hold for CH<sub>4</sub>. Alkanes, like isoprene, are removed mainly by reaction with OH. Whereas isoprene is emitted in large quantities by vegetation and reacts very quickly with OH, terpenes, also derived from natural sources, are to a greater extent degraded by other oxidation reactions, induced by O<sub>3</sub>.

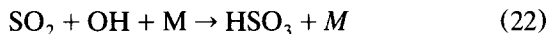
In addition to organic compounds, inorganic molecules such as NO<sub>2</sub> and sulphur dioxide are

Table 3:  
The global budgets of tropospheric trace gases and the fraction of each removed by oxidation with OH.

Trace gas	Annual production (million tons/year)	%Removal by oxidation with OH
CO	2800	90 <sup>a</sup>
CH <sub>4</sub>	500	90 <sup>b</sup>
Ethane	20	90 <sup>c</sup>
Isoprene	350	90 <sup>d,h</sup>
Terpenes ( $\alpha$ -pinene)	480	50 <sup>d,h</sup>
NO <sub>2</sub>	160	50 <sup>e</sup>
SO <sub>2</sub>	300	30 <sup>f</sup>
(CH <sub>3</sub> ) <sub>2</sub> S	50	90 <sup>g</sup>
CFCl <sub>3</sub>	0.2	0

<sup>a</sup>Volz et al. (1981); <sup>b</sup>Ehhalt (1974); <sup>c</sup>Ehhalt and Rudolph (1984); <sup>d</sup>Zimmermann et al. (1978); <sup>e</sup>Logan (1983); <sup>f</sup>Janßen-Schmidt et al. (1981); <sup>g</sup>Global Tropospheric Chemistry (1984); <sup>h</sup>Atkinson et al. (1984). The mean global OH concentration was taken as  $0.6 \times 10^6 \text{ cm}^{-3}$  (Volz et al., 1981).

also removed by reactions with OH. In both instances, however, other removal processes, in particular dry deposition at the earth's surface, are also important. Atmospheric oxidation by OH leads to acidic molecules: the oxidation of NO<sub>2</sub> (Eq. 21) leads to the formation of nitric acid. For SO<sub>2</sub>, the reaction sequence:



leads to the formation of sulfuric acid, H<sub>2</sub>SO<sub>4</sub>, which, because of its low vapour pressure, quickly attaches to aerosol particles. Needless to say, this reaction sequence also cycles OH to HO<sub>2</sub>. Sulfur dioxide, because of its ready solubility, also undergoes wet chemical oxidation in cloud droplets and precipitation. As a consequence the contribution of OH to its global removal is only ~30%.

In the case of NO<sub>2</sub>, night-time removal attributable to (a) oxidation to NO<sub>3</sub>, (b) conversion to N<sub>2</sub>O<sub>5</sub> and (c) heterogeneous removal of the two higher oxides on aerosol particles, provides another pathway for the loss of NO<sub>x</sub>, reducing the global contribution of OH to its removal by about 50%.

Only a few tropospheric trace gases escape oxidation by OH. These gases usually have no other tropospheric sinks and therefore are eventually mixed into the stratosphere, where they are photolysed by solar UV radiation. Among these are the chlorofluoromethanes which are exclusively man-made, and contribute to a reduction of the ozone layer. They provide an interesting example of the unexpected consequences which may result when a tropospheric trace gas cannot be removed by reaction with OH.

## 5. Conclusions

It was intended that this paper would demonstrate the great importance of OH for the self-cleansing capacity of the troposphere. Huge amounts of gases are processed by the tropospheric OH chemistry (see Table 3). It appears that the chemical system controlling OH in the relatively clean atmosphere is reasonably well un-

derstood; atmospheric environments with a complex mix of organic trace gases still need more research. The tropospheric OH concentrations are relatively insensitive to concentration changes in those gases that control OH as long as they remain relatively low in concentration. This is not always true in regional systems, where large fluxes of these gases can lower the local OH concentration considerably. Indeed, there are even indications that the average concentrations of OH in the global troposphere may have changed (Prinn et al., 1992).

## 6. References

- Atkinson, R., S.M. Aschmann, A.M. Winer and J.N. Pitts, Jr. 1984. Kinetics of gas phase reactions of NO<sub>3</sub> radicals with a series of dialkenes, cyclo-alkenes, and monoterpenes at 295 ± 1 K. *Environ. Sci. Technol.*, 18: 370–375.
- Callies, J., 1988. Absorptionsspektroskopischer Nachweis von Hydroxyl-Radikalen in der Troposphäre. Dissertation, University of Cologne.
- DeMore, W.B., J.J. Margitan, M.J. Molina, R.T. Watson, D.M. Golden, R.F. Hampson, M.J. Kurylo, C.J. Howard and A.R. Ravishankara, 1985. Chemical Kinetics and Photochemical Data for Use in Stratospheric Modeling, Evaluation 7, NASA Panel for Data Evaluation, JPL Publication, 85–37.
- Dorn, H.-P., J. Callies, U. Platt and D.H. Ehhalt, 1988. Measurements of tropospheric OH concentrations by laser long-path absorption spectroscopy. *Tellus* 40B: 437–445.
- Ehhalt, D.H. 1974. The atmospheric cycle of methane. *Tellus*, 26: 58–70.
- Ehhalt, D.H. 1989. Measurements of OH; an experiment designed to test theories of tropospheric gas phase chemistry. Plenary Lecture, International Conference on the Generation of Oxidants on Regional and Global Scales, Norwich, England, 3–7 July 1989.
- Ehhalt, D.H., H.-P. Dorn and D. Poppe, 1991. The chemistry of the hydroxyl radical in the troposphere. *Proc. R. Soc. Edinburgh*, 97B: 17–34.
- Ehhalt, D.H. and J. Rudolph, 1984. On the Importance of Light Hydrocarbons in Multiphase Atmospheric Systems. *Berichte der Kernforschungsanlage Jülich GmbH*, JUL-1942.
- Global Tropospheric Chemistry, A Plan for Action, 1984. National Academy Press, Washington, DC.
- Hough, A.M., 1988. An intercomparison of mechanisms for the production of photochemical oxidants. *J. Geophys. Res.*, 93: 3789–3812.
- Hübner, G., D. Perner, U. Platt, A. Toenissen and D.H. Ehhalt, 1984. Ground level OH radical concentration: new measurements by optical absorption. *J. Geophys. Res.*, 89: 1309–1319.

- Janßen-Schmidt, Th., E.P. Röth, G. Varhelyi and G. Gravenhorst, 1981. Anthropogene Anteile am atmosphärischen Schwefel- und Stickstoff-kreislauf und mögliche globale Auswirkungen auf chemische Umsetzungen in der Atmosphäre. Berichte der Kernforschungsanlage Jülich GmbH, JUL-1722.
- Junkermann, W., U. Platt and A. Volz-Thomas, 1989. A photoelectric detector for the measurement of photolysis frequencies of ozone and other atmospheric molecules, *J. Atmos. Chem.*, 8: 203–227.
- Logan, J.A., 1983. Nitrogen oxides in the troposphere: global and regional budgets. *J. Geophys. Res.*, 88: 10.785–10.807.
- Martin, R.S., H. Westberg, E. Allwine, L. Ashmau, J.C. Farmer and B. Lamb, 1991. Measurement of isoprene and its atmospheric oxidation products in a central Pennsylvania deciduous forest. *J. Atmos. Chem.*, 13: 1–22.
- Mozurkewich, M., P.H. McMurry, A. Gupta and J.G. Calvert, 1987. Mass accommodation coefficient for NO<sub>2</sub> radicals on aqueous particles, *J. Geophys. Res.*, 92: 4163–4170.
- Perner, D., U. Platt, M. Trainer, G. Hübler, J. Drummond, W. Junkermann, J. Rudolph, B. Schubert, A. Volz and D.H. Ehhalt, 1987. Measurements of tropospheric OH concentrations: a comparison of field data with model predictions. *J. Atmos. Chem.*, 5: 185–216.
- Platt, U., M. Rateike, W. Junkermann, J. Rudolph and D.H. Ehhalt, 1988. New tropospheric OH measurements. *J. Geophys. Res.*, 93: 5159–5166.
- Prinn R., D. Cunnold, P. Simmonds, R. Alyea, R. Boldi, A. Crawford, P. Fraser, D. Gutzler, D. Hartley, R. Rosen and R. Rasmussen, 1992. Global average concentration and trend for hydroxyl radicals deduced from ALE/GAGE trichloroethane (methyl chloroform) data for 1978–1990. *J. Geophys. Res.*, 97: 2445–2461.
- Spiegel, M.R., 1975. *Probability and Statistics*, McGraw Hill, New York.
- Stockwell, W.R., P. Middleton, J.S. Chang and X. Tang, 1990. The RADM II chemical mechanism for regional air quality modeling. *J. Geophys. Res.*, 95: 16343–16367.
- Thompson, A.M. and R.J. Cicerone, 1986. Possible perturbations to atmospheric CO, CH<sub>4</sub> and OH. *J. Geophys. Res.*, 91: 10853–10864.
- Volz, A., D.H. Ehhalt and R.G. Derwent, 1981. Seasonal and latitudinal variations of <sup>14</sup>CO and the tropospheric concentration of OH radicals. *J. Geophys. Res.*, 86: 5163–5171.
- Zimmermann, P.R. Fishmann, J. Chatfield, P.J. Crutzen and P.L. Hanst, 1978. Estimates of the production of CO and H<sub>2</sub> from the oxidation of hydrocarbon emissions from vegetation. *Geophys. Res. Lett.*, 5: 679–682.